ELSEVIER

Chemical Engineering Science 60 (2005) 4423–4430

Chemical Engineering Science

www.elsevier.com/locate/ces

Heat transfer phenomena in a solid oxide fuel cell: An analytical approach

F.A. Coutelieris*, S.L. Douvartzides, P.E. Tsiakaras

Department of Mechanical and Industrial Engineering, University of Thessalia, Pedion Areos, 38334 Volos, Greece

Received 28 May 2003; received in revised form 25 January 2005; accepted 10 March 2005
Available online 3 May 2005

Abstract

The steady-state heat transfer problem within a fuel cell is considered here. The original 2-D problem is defined while an averaging technique is used in order to reduce its dimensions to one. The full heat transfer equations along the appropriate boundary conditions are analytically solved for both solid and gas phase. Moreover, analytical expressions for the local as well as for the overall heat transfer coefficients are obtained. The gas temperature increases with the distance and the current density, while the temperature of the cell is always of so low variation that can be considered as a constant. Finally, the heat transfer coefficient presents a profile reverse to that of gas temperature.

Keywords: Fuel cell; Heat transfer; Conduction; Convection; Mathematical modeling; Laminar flow

1. Introduction

One of the most promising new technologies in the sector of electrical power systems is that of fuel cells, whose concept has been known for more than a century. Being electrochemical energy conversion devices, the major product of fuel cells is electrical power while their impact on atmosphere quality is zero or near zero. Additionally, the replacement of spontaneous combustion of the typical heat engines with controllable electrochemical oxidation moderates the production of pollutants in the fuel gases. Since the by-products of the electrochemical reaction in a fuel cell are water and a significant amount of heat, effective thermal management is one of the important problems for all the types of fuel cells (Appleby and Foulkes, 1989; Kordesh and Simander, 1996).

Among the different types of fuel cells, solid oxide fuel cells (SOFCs) that are solid state, ceramic cells operating currently at high temperatures, present special interest because of the flexibility in fuel choice due to high operation temperature (Virkar et al., 1997). Since a SOFC stack consists of many connected cells, stack models can be built upon the conventional heat balance equations but further consideration of electrochemical reaction and its consequences should be also taken into account. Usually, the cell stack models require consideration of gas flow, heat transfer, mass transfer, and cell voltage–current relationship. Some mathematical models (e.g. molecular dynamics approach, stochastic models, etc.) need several geometrical and electrochemical parameters, which are functions of temperature and gas composition (Dutta et al., 2001; Koh et al., 2001). Theoretical prediction of temperature distribution is important for SOFC stack design and its stable operation, and it should be achieved by solving a rigorous mathematical model.

A lot of investigations concerning mathematical modeling have been presented in order to adequately simulate the heat transfer within SOFCs. The majority of SOFC thermal models pertain to the planar and monolithic designs (Minh and Takahashi, 1995). Ahmed et al. (1991) assumed fully developed laminar flow presenting Nusselt number value of 3 for convective heat transfer. Bassette et al. (1995) also presented a thermal model of a tubular SOFC design having limited validation to one experimental datum. Kanamura et al. (1989) and Hirano et al. (1992) presented

* Corresponding author at: National Center for Scientific Research, "Demokritos", 15310 Aghia Paraskevi Attikis, Greece. Tel./fax: +302106525004.
E-mail address: frank@ipta.demokritos.gr (F.A. Coutelieris).

0009-2509/$ - see front matter © 2005 Elsevier Ltd. All rights reserved.
doi:10.1016/j.ces.2005.03.013

also thermal models and simulations but of limited electrochemical validation.

This work presents an analytical model for the thermal transport phenomena occurred within a SOFC stack operating at high temperatures. By considering the complete conduction–convection heat transfer equation along the cell, analytical expressions for the spatial distribution of both the gas and the cell temperatures as well as for the local and overall heat transfer coefficient are obtained by using an averaging technique. As the modeled fuel cell is a real cylindrical design and the electrochemistry considered is quite complete, the basic barriers mentioned above are overcome and the use of these analytical formulas can be very helpful in the design and/or in the operating phase of such systems, as the produced results are sufficiently accurate for any practical application.

2. Formulation of the problem

A typical fuel cell stack consists of an anode and a cathode part between which a catalyst (electrolyte) layer exists. The atmospheric air flows in the cathode "area" (gas channel) while the anode is exposed to hydrogen. The present model studies a compatible to the Siemens–Westinghouse cylindrical fuel cell design (George and Bassette, 1998; Hirschenhofer et al., 1998) as it is illustrated in Fig. 1a. By considering the simplest and most studied reaction of hydrogen oxidation in the presence of oxygen (air), one might have the formation of water with heat and electricity production, as follows (Koh et al., 2001):

$$H_2 + \tfrac{1}{2}O_2 \rightarrow H_2O + \text{heat} + \text{electricity}. \tag{1}$$

The area of interest is the cylinder ABCD of Fig. 1a, which is presented in detail in Fig. 1b. By assuming

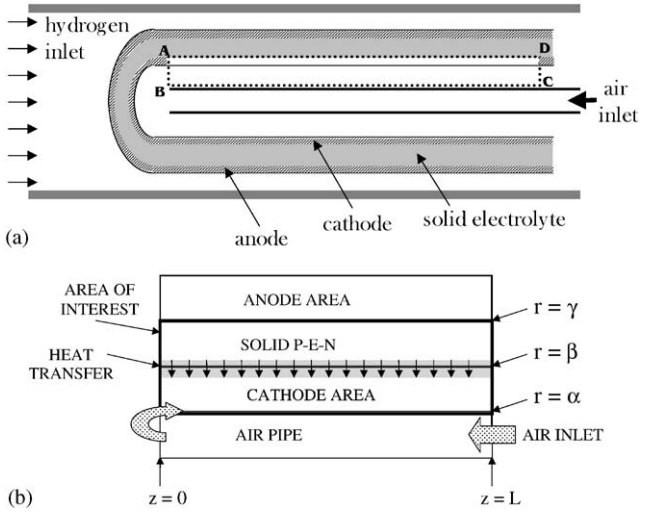

Fig. 1. Design of a tubular fuel cell (a) and blow up of the area of interest (b).

axial symmetry and fully developed incompressible laminar flow and by ignoring heat transfer due to radiation, the conduction–convection heat transport equations can be written as follows:

$$u_z(r)\frac{\partial T_g(r,z)}{\partial z} = \alpha_f\left(\frac{\partial^2 T_g(r,z)}{\partial r^2} + \frac{1}{r}\frac{\partial T_g(r,z)}{\partial r} + \frac{\partial^2 T_g(r,z)}{\partial z^2}\right), \tag{2a}$$

$$s(z) = \alpha_s\left(\frac{\partial^2 T_c(r,z)}{\partial r^2} + \frac{1}{r}\frac{\partial T_c(r,z)}{\partial r} + \frac{\partial^2 T_c(r,z)}{\partial z^2}\right), \tag{2b}$$

where $T_g(r,z)$ and $T_c(r,z)$ are the gas and solid temperature, respectively, $u_z(r)$ is the z-component of the fluid velocity and α_f and α_s are thermal diffusivities in the fluid and the solid phase, respectively.

The above equation can be integrated with the following boundary conditions:

$$T_g(r,0) = \text{const.}, \quad \alpha \leqslant r \leqslant \beta, \tag{3a}$$

$$\left.\frac{\partial T_g(r,z)}{\partial z}\right]_{z=L} = 0, \quad \alpha \leqslant r \leqslant \beta, \tag{3b}$$

$$\left.\frac{\partial T_g(r,z)}{\partial r}\right]_{r=\alpha} = 0, \quad 0 \leqslant z \leqslant L, \tag{3c}$$

$$\left.\frac{k(z)}{\rho c_p}\frac{\partial T_g(r,z)}{\partial r}\right]_{r=\beta} = s(z), \quad 0 \leqslant z \leqslant L, \tag{3d}$$

$$T_c(r,0) = \text{const.}, \quad \beta \leqslant r \leqslant \gamma, \tag{3e}$$

$$\left.\frac{\partial T_c(r,z)}{\partial z}\right]_{z=L} = 0, \quad \beta \leqslant r \leqslant \gamma, \tag{3f}$$

$$\left.\frac{\partial T_c(r,z)}{\partial r}\right]_{r=\gamma} = 0, \quad 0 \leqslant z \leqslant L \tag{3g}$$

and

$$T_g(\beta,z) = T_c(\beta,z), \quad 0 \leqslant z \leqslant L. \tag{3h}$$

Boundary conditions (3a) and (3e) insure a constant profile for the gas and solid temperature at the inlet while Eqs. (3b) and (3f) imposes typical von Newman conditions for the outlet temperature. Eqs. (3c) and (3g) are proposed in order to ensure the continuity of the temperature upon the outer boundaries of the area of interest while Eq. (3h) imposes the continuity of the temperature on the gas–solid interface. Finally, Eq. (3d) expresses the transport to the cathode gas of the heat produced upon the electrodic material surface due to electrochemical reaction (1).

By $s(z)$ in Eq. (2b), is denoted the spatial distribution of the heat sources along the cell in the cross-section z, defined as

$$s(z) = j(U_t + jr_{\text{eff}} - E(z)), \tag{4}$$

where j is the current density, which is assumed to be constant, as previous investigations have shown that it presents low variability for the conditions considered here (Koh et al., 2001, Djilali and Lu, 2002). By U_t is denoted the thermo neutral voltage:

$$U_t = \frac{-\Delta H_{H_2}}{2F} \approx 1.29\,\text{V}. \tag{5}$$

Finally, the effective specific resistance of the cell, r_{eff}, includes the ohmic, the polarization anodic and the polarization cathodic resistances, according to the relation (Haynes and Wepfer, 2000):

$$r_{\text{eff}} = r_{\text{ohm}} L + r_{\eta a} + r_{\eta c}. \tag{6}$$

Although the above formulation is rather obvious from transport processes point of view, the solution of the consequent boundary value problem is difficult as it includes sometimes circular schemes. This difficulty is the main reason for the lack of analytical and/or numerical solutions of such type of formulations as well as for the mathematical manoeuvres used in the literature (Dutta et al., 1997; Yuan et al., 2001; Haynes and Wepfer, 2001; Yuan and Sunden, 2004).

3. Problem simplification and solution

By considering a circular ring of the domain of the interest, it is easy to define an averaging procedure in a cross-section z, as it is presented in Fig. 2. In that case, the original two-dimensional gas temperatures, $T_g(r, z)$ and $T_c(r, z)$, become

$$T_g(z) = \frac{1}{\beta - \alpha} \int_{\alpha}^{\beta} T_g(r, z) 2\pi r \, \mathrm{d}r, \tag{7a}$$

$$T_c(z) = \frac{1}{\gamma - \beta} \int_{\beta}^{\gamma} T_c(r, z) 2\pi r \, \mathrm{d}r. \tag{7b}$$

This averaging procedure should be applied separately in the solid and the gas phase, in order to avoid missing of information about the heat sources upon the solid–gas interface. Therefore, it is necessary for the heat transfer equation to be considered in both the two different shrinking phases.

As the conduction is the only available mechanism for the heat transport within solids, the heat transfer in the solid phase of the cell is described by the following differential equation:

$$-\alpha_s \frac{\mathrm{d}^2 T_c(z)}{\mathrm{d}z^2} = s(z), \tag{8}$$

where α_s denotes the thermal diffusivity within the solid phase.

The electromotive force at position z for a mean cell temperature value $\langle T_c(z)\rangle$, averaged along the length of the cell, is given by Tsiakaras and Demin (2001)

$$E(z) = \frac{R\langle T_c(z)\rangle}{4F} \ln \frac{0.209}{[y_{H_2O}/y_{H_2} K]^2}, \tag{9}$$

where

$$\langle T_c(z)\rangle = \frac{1}{L} \int_0^L T_c(z) \, \mathrm{d}z \tag{10}$$

or, by using dimensionless quantities,

$$\langle T_c(x)\rangle = \int_0^1 T_c(x) \, \mathrm{d}x, \tag{11}$$

where $x = z/L$. The symbol K in Eq. (9) denotes the equilibrium constant of reaction (1). The utilization factor (extent of reaction), η_f, is defined as

$$\eta_f = \frac{p_{H_2}(0) - p_{H_2}(1)}{p_{H_2}(0)}. \tag{12}$$

As the fuel is almost pure hydrogen, it can be highly utilized and, therefore, η_f is set to 0.85 as $p_{H_2}(0) = 0.98$ and $p_{H_2}(1) = 0.15$ (Demin and Tsiakaras, 2001). After introducing the utilization factor, a suitable expression for the

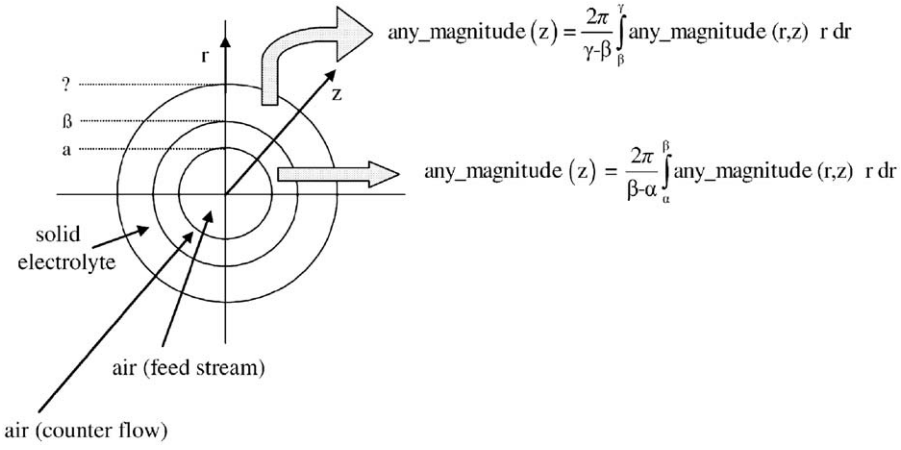

Fig. 2. Reduction of the problem's dimensions.

electromotive force can be obtained:

$$E(x) = \frac{R\langle T_c(x)\rangle}{4F} \times \left(\ln 0.209K^2 - 2 \ln \frac{p_{H_2}(0)(1-\eta_f x)}{1-p_{H_2}(0)(1-\eta_f x)} \right). \quad (13)$$

After some simple mathematical manipulations, Eq. (8) can be written as

$$\frac{d^2T_c(x)}{dx^2} = a_0 + a_1 \ln \left(\frac{p_{H_2}(0)(1-\eta_f x)}{1-p_{H_2}(0)(1-\eta_f x)} \right), \quad (14)$$

where

$$a_0(\langle T_c(x)\rangle) = -\frac{j}{\alpha_s}\left[U_t + jr_{\text{eff}} - \frac{R\langle T_c(x)\rangle}{4F} \ln 0.209K^2 \right] \quad (15a)$$

and

$$a_1(\langle T_c(x)\rangle) = \frac{jR\langle T_c(x)\rangle}{2\alpha_s F}. \quad (15b)$$

The general solution of Eq. (14), which contains two real arbitrary constants C_1 and C_2, is of the form:

$$T_c(x) = a_0x^2 + a_1\frac{(1-2\eta_f x)}{2\eta_f^2} \ln[p_{H_2}(0)(1-\eta_f x)] - a_1\frac{(1-p_{H_2}(0))^2(1-\eta_f x)}{2[p_{H_2}(0)]^2\eta_f^2} \times \ln[1-p_{H_2}(0)(1-\eta_f x)] + \frac{a_1}{2}x^2 \ln\left[\frac{p_{H_2}(0)(1-\eta_f x)}{1-p_{H_2}(0)(1-\eta_f x)}\right] + C_1x + C_2. \quad (16)$$

The cell surface is assumed to be quasi-isothermal (Haynes and Wepfer, 2000; Yuan et al., 2001):

$$T_c(1) = T_c(0) \quad (17a)$$

while a standard Dirichlet condition is used for describing the temperature profile at inlet (Murugesamoorti et al., 1993):

$$T_c(0) = \text{constant}. \quad (17b)$$

By concerning the above boundary conditions, the arbitrary constants of Eq. (16) are identified as follows:

$$C_1 = \frac{a_1 \ln[p_{H_2}(0)]}{2\eta_f^2} - \frac{a_1(1-2\eta_f)}{2\eta_f^2} \times \ln[p_{H_2}(0)(1-\eta_f)] - a_0 - \frac{a_1(1-p_{H_2}(0))^2}{2[p_{H_2}(0)]^2\eta_f^2} \ln[1-p_{H_2}(0)] + a_1\frac{(1-p_{H_2}(0))^2(1-\eta_f)}{2[p_{H_2}(0)]^2\eta_f^2} \times \ln[1-p_{H_2}(0)(1-\eta_f)] - \frac{a_1}{2} \ln\left[\frac{p_{H_2}(0)(1-\eta_f)}{1-p_{H_2}(0)(1-\eta_f)}\right], \quad (18a)$$

$$C_2 = T_c(0) - \frac{a_1 \ln[p_{H_2}(0)]}{2\eta_f^2} + \frac{a_1(1-p_{H_2}(0))^2}{2[p_{H_2}(0)]^2\eta_f^2} \times \ln[1-p_{H_2}(0)]. \quad (18b)$$

In the gas phase the governing differential equation for the heat transfer is

$$u(x)\frac{dT_g(x)}{dx} = \alpha_f \frac{d^2T_g(x)}{dx^2}. \quad (19)$$

By involving the constant mass flow rate of the gas, $\dot{m}$, through a circular surface of diameter d, and by assuming that the atmospheric air behaves as a perfect gas flowing under fully developed incompressible laminar flow conditions, the velocity $u(x)$ can be expressed by the well-known Hagen–Poiseuille flow as (Bird et al., 1960)

$$u(x) = \frac{4\dot{m}}{\pi d^2}. \quad (20)$$

It is worth noticing that the viscosity of the atmospheric air (gas mixture) is necessary to be constant in order to use Eq. (20), but viscosity is in general an unknown function of the gas temperature. However, it has been presented that the variation of air viscosity is less than 4% per 25 K (Perry and Green, 1997) and, thus, it can be considered as constant for variation of gas temperature up to 100 K. On the other hand, high-temperature differences may destroy the material of the solid electrolyte and this is another reason for keeping the temperature differences up to 100 K.

The differential equation describing the heat transfer in the gas phase becomes

$$\frac{4\dot{m}}{\pi d^2}\frac{dT_g(x)}{dx} = \alpha_f \frac{d^2T_g(x)}{dx^2}. \quad (21)$$

The general solution of the above equation can be obtained easily and is of the form:

$$T_g(x) = C_3\frac{\pi d^2\alpha_f}{4\dot{m}} e^{(4\dot{m}/\pi d^2\alpha_f)x} + C_4. \quad (22)$$

By employing the boundary conditions:

$$T_g(1) - T_g(2) = \Delta T_g \tag{23a}$$

and (Demin and Tsiakaras, 2001)

$$T_g(0) = \text{constant and close to } T_c(0) \tag{23b}$$

the above-mentioned arbitrary constants are identified as

$$C_3 = \frac{4\Delta T_g \dot{m}}{\pi d^2 \alpha_f (1 - e^{(4\dot{m}/\pi d^2 \alpha_f)})}, \tag{24a}$$

$$C_4 = T_g(0) - \frac{\Delta T_g}{1 - e^{(4\dot{m}/\pi d^2 \alpha_f)}}. \tag{24b}$$

By employing the specific flux of the heat absorbed by the cathode gas, the temperature of the cell, $T_c(x)$, is related to the gas temperature as follows:

$$j(U_t + jr_{\text{eff}} - E(x)) = h(x)(T_c(x) - T_g(x)) \tag{25}$$

and, therefore, the local heat transfer coefficient, $k(x)$, can be calculated. The overall heat transfer coefficient k_0 can be estimated as

$$h_0 = \int_0^1 h(x)\,\mathrm{d}x = j\int_0^1 \frac{U_t + jr_{\text{eff}} - E(x)}{T_c(x) - T_g(x)}\,\mathrm{d}x. \tag{26}$$

Finally, the mass flow rate can be calculated by using the macroscopic balance for the heat absorbed by gas:

$$\dot{m} = \frac{Q}{c_p\,\Delta T_g} = \frac{\pi d j(U_t + jr_{\text{eff}} - \langle E\rangle)}{c_p\,\Delta T_g}, \tag{27}$$

where Q is the overall heat absorbed, $\langle E\rangle$ denotes averaging of $E(x)$ given by Eq. (13) along x, and c_p is the heat capacity of the atmospheric air. By assuming the standard environmental composition, c_p varies in a range of about 31–34 J/mol of atmospheric air for a given temperature range of 800–1200 K.

A generalized iterative scheme is necessary for the solution of the problem, as follows:

- guess an initial value for $\langle T_c(x)\rangle^{(\text{previous})}$;
- calculate a_0 and a_1 from Eqs. (15a) and (15b);
- estimate $T_c(x)$ from Eqs. (16), (18a) and (18b);
- find $\langle T_c(x)\rangle^{(\text{next})} = \int_0^1 T_c(x)\,\mathrm{d}x$;
- if $\langle T_c(x)\rangle^{(\text{next})} = \langle T_c(x)\rangle^{(\text{previous})}$ stop the procedure as the solution is $T_c(x)$ estimated at Step2; otherwise set $\langle T_c(x)\rangle^{(\text{previous})} = \langle T_c(x)\rangle^{(\text{next})}$ and repeat Step2–Step5;
- calculate $T_g(x)$ from Eqs. (22), (24a) and (24b);
- estimate h_0 from Eq. (26).

4. Results and discussion

As it is senseless for a general theoretical study to fix values for thermal diffusivities of the solid electrolyte, the ratio of α_s/α_f is used instead of α_s and it is adjusted to 10,000 because it is known that gases are bad heat conductors. Thermal diffusivities of atmospheric air at various temperatures are taken from the appropriate published tables (Perry and Green, 1997).

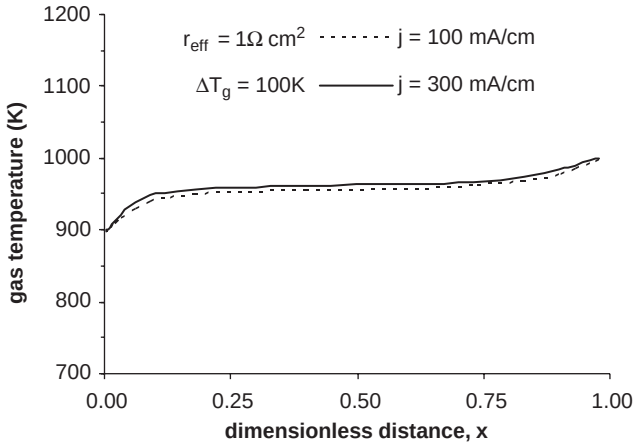

Fig. 3. Spatial distribution of the gas temperature for various current densities.

4.1. Gas temperature, T_g

The distribution of the gas temperature along the dimensionless length of the cell is presented in Fig. 3 for two typical values of current density (100 and 300 mA/cm^2). The specific effective resistance is 1 Ω cm^2 and the temperature difference in the gas phase, ΔT_g, has been fixed to 100 K. This value for the temperature difference has been chosen to be low enough to insure that the viscosity does not change significantly and, therefore, the Hagen–Poiseuille flow regime is valid. In general, the higher temperature is calculated in the outlet of the cell, as the moving air absorbs heat and, therefore, its temperature increases as x approaches 1. The very high slope of the profiles presented at narrow area near inlet is due to some numerical limitations in the calculation of electromotive force at this area and is of senseless physical meaning. Finally, a small variable decrement (up to 1.2%) of the gas temperature with increment of current density is observed. Although a direct dependence of $T_g(x)$ on j is not obvious, it exists through the molar flow rate $\dot{m}$, which depends on the current density (see discussion below). The gas temperature depends on $\dot{m}$ exponentially in a complicated manner (see Eqs. (22), (24a) and (24b)) of the form $(e^{x-1})^{\dot{m}}$. As $x \leqslant 1$, an increment of $\dot{m}$ corresponds to lower values of $(e^{x-1})^{\dot{m}}$ and, therefore, the small decrement occurs.

Fig. 4 shows the distribution of the gas temperature along the stack's length for two typical values of temperature difference in the gas phase ($\Delta T_g = 50$ and 100 K). The specific effective resistance is again 1 Ω cm^2 and the current density j has been fixed to 100 mA/cm^2. According to the results

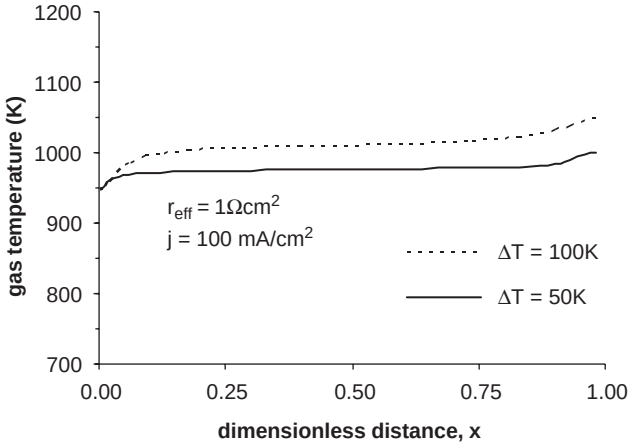

Fig. 4. Profiles of the gas temperature for various ΔT_g.

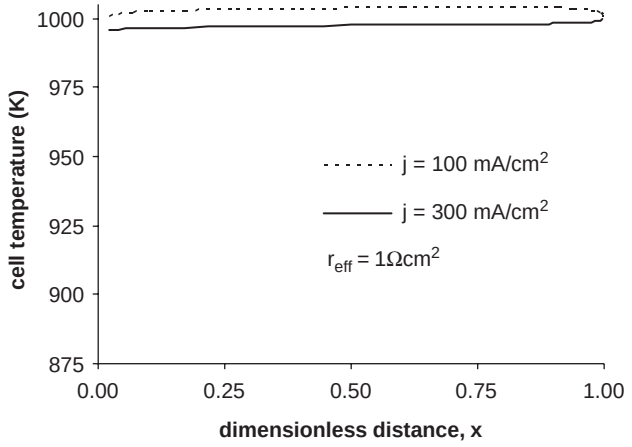

Fig. 5. Dependence of the cell temperature on the current density.

presented in Fig. 3, the gas temperature presents its lower values in the inlet area while it increases as x approaches the outlet area. Obviously, higher ΔT_g correspond to higher the curves of the gas temperature. Finally, it is worth noticing that the second derivative of $T_g(x)$ is of three to four orders of magnitude lower than the first one in all cases. Additionally, $\mathrm{d}^2T_g(x)/\mathrm{d}x^2$ is multiplied by the small number α_f and the final product becomes even smaller. This underlines the negligible character of conduction in the gas phase because of the high Peclet flow of the atmospheric air in the cathode area.

4.2. Cell temperature, T_c

The profile of the cell temperature is presented in Fig. 5 for conditions quite analogous to those of Fig. 3 ($j = 100$ and $300\,\mathrm{mA/cm^2}$, $r_{\mathrm{eff}} = 1\,\Omega\,\mathrm{cm^2}$). As $T_c(0) = T_c(1)$, the spatial variation of $T_c(x)$ is always less than 0.5% for any current and resistance (it corresponds to an absolute value of 5 K with respect to the 1000 K of operational temperature), which means that it could be accurately considered as constant, as it has been previously reported in the related bibliography (Haynes and Wepfer, 2001). More precisely, there are some combinations of resistances and currents where the cell temperature presents a really constant profile with maximum absolute divergence from the base line less than 0.0025%. Finally, it should be noted that $T_c(x)$ is independent on ΔT_g as it can obviously derived from Eqs. (15a), (15b), (16), (18a) and (18b). It should be also stressed out that, in general, $T_g(x) \neq T_c(x)$, which can be interpreted as a discontinuity on the gas–solid interface of the gas temperature as it had been defined in the real problem (see Section 2). In fact, it is a reckless and false conclusion as the interface clearly loses its physical meaning after applying the averaging procedure presented above.

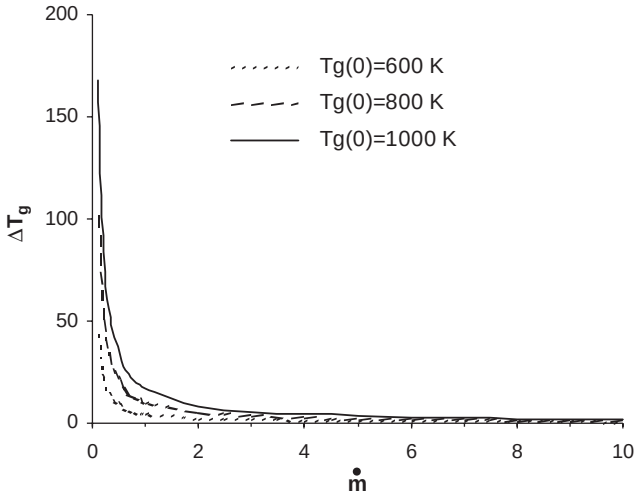

Fig. 6. Relation between the temperature difference and the mass flowrate.

4.3. Molar flow rate, $\dot{m}$

Obviously from Eq. (27), the influence of j on $\dot{m}$ is of parabolic form. In general, higher current densities correspond to higher amounts of heat produced in the electrolyte due to Joule phenomenon and, thus, to higher flow rates of the cathode gas in order to obtain complete heat transfer from the electrolyte to gas phase. Furthermore, $\dot{m}$ depends on ΔT_g in a reversibly analogous manner for constant j. This influence is presented in Fig. 6 for $j = 100\,\mathrm{mA/cm^2}$, $r_{\mathrm{eff}} = 1\,\Omega\,\mathrm{cm^2}$ and various initial temperatures $T_g(0)$. In terms of physics, the temperature difference in the gas phase represents the "flexibility" of the gas in thermal absorption and, thus, lower values of ΔT_g correspond to higher flow rates, as the total heat amount should be completely absorbed by gas.

4.4. Local heat transfer coefficient, $h(x)$

Fig. 7 presents the spatial profile of the local heat transfer coefficient, $h(x)$, defined by Eq. (25) as a function of

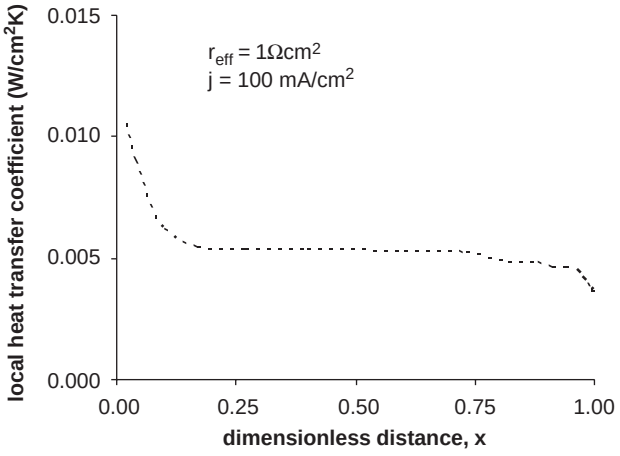

Fig. 7. Spatial distribution of the heat transfer coefficient.

the dimensionless distance for typical values of specific effective resistance and current density ($r_{\text{eff}} = 1\,\Omega\,\text{cm}^2$ and $j = 100\,\text{mA/cm}^2$). In agreement to previously presented results (Koh et al., 2001), the local heat transfer coefficient is almost constant for a wide domain along the cell except the inlet and outlet areas, where the end-effects force the convection thermal film to attain its bulk values. Additionally to this purpose, the above-mentioned numerical limitation in the calculation of electromotive force at $x = 0$ influence significantly to the modulation of such a sharp slope in the heat transfer coefficient profile.

5. Conclusions

The steady-state heat transfer problem from the solid electrolyte to the absorbing cathode gas within a fuel cell was considered here. After a reduction of the dimensions of the original problem by using an averaging technique, the heat transfer equations accompanied by the appropriate boundary conditions solved analytically for both the solid and gas phases. Analytical expressions for the local and the overall heat transfer coefficient were also obtained. It was found that the cell temperature varied low enough to be considered as constant. Finally, the overall heat transfer coefficient was found to present a profile reverse to that of gas temperature.

Notation

a_0, a_1	constants defined by Eqs. (15a) and (15b), respectively
c_p	heat capacity at constant pressure
C_1, C_2, C_3, C_4	integration constants defined by Eqs. (18a), (18b), (24a) and (24b), respectively
d	diameter of the cell
$E(x)$	electromotive force at position x
$\langle E \rangle$	overall electromotive force
F	Faradays' constant (=96, 484 J/mol V)
$h(x)$	local heat transfer coefficient at position x
h_0	overall heat transfer coefficient
j	current density per unit area
$k(z)$	thermal conductivity
K	equilibrium constant of reaction (1)
L	length of the cell stack
$\dot{m}$	cathode gas mass flow rate
$p_{\text{H}_2}(x)$	partial pressure of hydrogen at position x
Q	overall heat absorbed by gas
r, z, θ	cylindrical spatial coordinates
r_{eff}	effective specific resistance
r_{ohm}	ohmic resistance
$r_{\eta a}, r_{\eta c}$	polarization anodic and cathodic resistance
R	universal gas constant (=8.314 J/mol K)
$s(x)$	heat sources at position x
T_c, T_g	cell and gas temperature, respectively
$u(x)$	one-dimensional fluid velocity at position x
$u_z(r)$	z-component of the fluid velocity at position r
U_t	thermoneutral voltage
x	dimensionless spatial coordinate($=z/L$)
$y_{\text{H}_2}, y_{\text{H}_2\text{O}}$	molar fractions of hydrogen and water, respectively

Greek letters

α, β, γ	radius of the air pipe, the cathode area and the electrolyte cylinder, respectively
α_s, α_f	thermal diffusivity in solid and fluid phase, respectively
$-\Delta H_{\text{H}_2}$	lower heating value (enthalpy of combustion) of hydrogen at standard conditions
ΔT_g	gas temperature difference used in Eq. (23a)
η_f	utilization factor defined by Eq. (12)
ρ	density of atmospheric air

References

Ahmed, S., McPheeters, C., Kumar, R., 1991. Thermal-hydraulic model of a solid oxide fuel cell. Journal of the Electrochemical Society 138, 2712.

Appleby, A.J., Foulkes, F.R., 1989. Fuel Cell Handbook. Van Norstand Reinhold, New York.

Bassette, N.F., Wepfer, W.J., Winnick, J., 1995. A mathematical model of a solid oxide fuel cell. Journal of the Electrochemical Society 142, 3792–3800.

Bird, R.B., Stewart, W.E., Lightfoot, E.N., 1960. Transport Phenomena. Wiley, New York.

Demin, A., Tsiakaras, P., 2001. Thermodynamic analysis of a hydrogen fed solid oxide fuel cell based on a proton conductor. International Journal of Hydrogen Energy 26, 1103–1108.

Djilali, N., Lu, D., 2002. Influence of heat transfer on gas and water transport in fuel cells. International Journal of Thermal Science 41, 29–40.

Dutta, S., Morehouse, J.H., Khan, J.A., 1997. Numerical analysis of laminar flow and heat transfer in a high temperature electrolyzer. International Journal of Hydrogen Energy 26, 883–895.

Dutta, S., Shimpalee, S., Van Zee, J.W., 2001. Numerical prediction of mass-exchange between cathode and anode channels in a PEM fuel cell. International Journal of Heat and Mass Transfer 44, 2029–2042.

George, R.A., Bassette, N.F., 1998. Reducing the manufacturing cost of tubular SOFC technology. Journal of Power Sources 71, 131–137.

Haynes, C.L., Wepfer, W.J., 2000. Design for power of a commercial grade tubular solid oxide fuel cell. Energy Conversion and Management 41, 1123–1139.

Haynes, C.L., Wepfer, W.J., 2001. Characterizing heat transfer within a commercial-grade tubular solid oxide fuel cell for enhanced thermal management. International Journal of Hydrogen Energy 26, 369–379.

Hirano, A., Suzuki, M., Ippommatsu, M., 1992. Evaluation of a new solid oxide fuel cell system by nonisothermal modeling. Journal of the Electrochemical Society 139, 2744–2751.

Hirschenhofer, J.H., Stauffer, D.B., Engelman, R.R., 1998. Fuel Cells: A Handbook (rev. 3). US DOE Office of Fossil Energy, Morgantown.

Kanamura, K., Shoji, Y., Zen-ichiro, T., 1989. Proceedings of the First International Symposium on SOFCs. Electrochemical Society, Pennigton.

Koh, J.-H., Seo, H.-K., Yoo, Y.-S., Lim, H.C., 2001. Consideration of numerical simulation parameters and heat transfer models for a molten carbonate fuel cell stack. Chemical Engineering Journal 3913, 1–13.

Kordesh, J.H., Simander, G., 1996. Fuel Cells and Their Applications. VCH Publishers, New York.

Minh, T.Q., Takahashi, T., 1995. Science and Technology of Ceramic Fuel Cells. Elsevier, Amsterdam.

Murugesamoorti, K.A., Srinivasan, S., Appleby, A.J., 1993. Research development and demonstration of SOFC systems. In: Blomen, L.J.M.J., Mugerwa, M.N. (Eds.), Fuel Cell Systems. Plenum Press, New York.

Perry, R.H., Green, D.W., 1997. Chemical Engineers Handbook. Seventh ed. McGraw-Hill, New York.

Tsiakaras, P., Demin, A., 2001. Thermodynamic analysis of a solid oxide fuel cell system fuelled by ethanol. Journal of Power Sources 102, 210–217.

Virkar, A.V., Fung, K., Singhal, S.C., 1997. DOE Report, DOE/GETC/C-98/7303, USA.

Yuan, J., Rokni, M., Sunden, B., 2001. Simulation of fully developed laminar heat and mass transfer in fuel cell ducts with different cross-sections. International Journal of Heat and Mass Transfer 44, 4047–4058.

Yuan, J., Sunden, B., 2004. Two-phase flow analysis in a cathode duct of PEFCs. Electrochimica Acta 50, 673–679.